Three dimensional seismic and static stability of rock slopes

X.L. Yang [*1,2] and Q.J. Pan [3a]

[1] *School of Civil Engineering, Central South University, Hunan 410075, China*
[2] *College of Civil Engineering, Fujian University of Technology, Fuzhou 350118, China*
[3] *Laboratory 3SR, Grenoble Alpes University, CNRS UMR 5521, Grenoble, France*

Abstract. The kinematical approach of limit analysis is used to estimate the three dimensional stability analysis of rock slopes with nonlinear Hoek-Brown criterion under earthquake forces. The generalized tangential technique is introduced, which makes limit analysis apply to rock slope problem possible. This technique formulates the three dimensional stability problem as a classical nonlinear programming problem. A nonlinear programming algorithm is coded to search for the least upper bound solution. To prove the validity of the present approach, static stability factors are compared with the previous solutions, using a linear failure criterion. Three dimensional seismic and static stability factors are calculated for rock slopes. Numerical results of indicate that the factors increase with the ratio of slope width and height, and are presented for practical use in rock engineering.

Keywords: Hoek-Brown criterion; limit analysis; rock slope; three dimensions

1. Introduction

As well known, Mohr-Coulomb (MC) failure criterion has been extensively used in stability analysis of rock engineering. This may be due to the fact that most computer codes, design practice and standards, which are currently employed for evaluating the stability of rock structures, are formulated in terms of a MC failure criterion. With the MC criterion, it is supposed that, on failure plane the relationship between normal and shearing stress is linear. However, much evidence shows that the strength envelops of almost all geomaterials are nonlinear (Agar *et al*. 1985, Cai 2007, Cai *et al*. 2007, Lade 1977). The friction angle decreases in most geomaterials with increasing confining pressure in tests, and Mohr's envelope is curved. In the past, many researches were performed on nonlinear failure criterion. Various strength envelopes were proposed to represent nonlinear strength envelopes. For example, a power law criterion was presented by Hobbs (1966) based on triaxial test and had been successful applied to stability analysis for mine tunnel. Ladanyi (1974) proposed a nonlinear failure criterion on the basis of Griffith crack theory. The well known Hoek-Brown (HB) failure criterion, concluded on the results for a large amount of rock test, is also nonlinear (Hoek and Brown 1980).

∗Corresponding author, Professor, E-mail: yangky@aliyun.com
[a] E-mail: panqiujing2013@gmail.com

Limit analysis is an effective approach to stability problem of geotechnical engineering, by which many scholars study the slope stability (Zhang *et al*. 2014, Zhu *et al*. 2010, 2011, 2012). However, these researches are mainly carried out based on plain strain analysis, with little utilization of three-dimensional (3D) analysis. Baligh and Azzouz (1975) considered a cylindrical and spherical mechanism and analyzed the stability of cohesive slope under undrained condition. Michalowski (1989) proposed a 3D multi-blocks mechanism, based on limit analysis method. The slip mass was divided into a series of blocks. For each of block, the velocity field was constructed in two-dimensional (2D) condition. Farzaneh and Askari (2003) applied this mechanism into the 3D stability of inhomogeneous slope. An effective iterative algorithm was discussed for searching the optimum least upper bound solutions. Furthermore, Michalowski and Drescher (2009) proposed a 3D mechanism reflecting the relationship between slope depth and stability factor, which was composed of a rotation mechanism and a plane insert mechanism. These 3D works are performed with a linear MC failure criterion. Consequently, a question, which often arises in practice and theoretical study, is how to determine 3D stability of rock slopes using a nonlinear failure criterion.

In the presented study, the 3D stability of rock slopes, subjected to earthquake forces, is analyzed with the nonlinear HB failure criterion. Earthquake forces, regarded as external forces, are calculated using a seismic coefficient. The upper bound theorem of limit analysis is applied to estimate the seismic and static stability problem of rock slopes. To avoid the difficulty resulting from the nonlinear HB failure criterion, generalized tangential technique is used to formulate the 3D stability problem as a classical nonlinear programming problem. A nonlinear programming algorithm is coded to search for the least upper bound solution. In order to see the validity of the presented approach, stability factors are compared with the solutions of Michalowski and Drescher (2009), when the nonlinear failure criterion reduces into MC one. This paper extends the work for calculation of the 3D static stability analysis using linear MC yield criterion by Michalowski and Drescher (2009) to that using nonlinear criterion under earthquake.

2. Generalized tangential technique

According to a large number of triaxial experiments on a variety of rock types with varying degrees of fracturing, failure criteria are nonlinear. Hoek and Brown presented a modified HB failure criterion, which can be described by the following equation (Hoek and Brown 1997, Hoek *et al*. 2002)

$$\sigma_1 - \sigma_3 = \sigma_c \left[\frac{m\sigma_3}{\sigma_c} + s \right]^n \tag{1}$$

where σ_1 and σ_3 are minimum and maximum principal stresses, and σ_c is the uniaxial compressive stress of the rock. The parameters *m*, *s*, *n* are defined as follows

$$\frac{m}{m_i} = \exp\left(\frac{GSI - 100}{28 - 14D} \right) \tag{2}$$
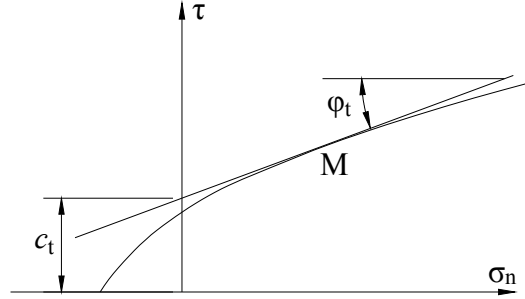
$$s = \exp\left(\frac{GSI - 100}{9 - 3D} \right) \tag{3}$$

Fig. 1 Tangential line to the modified Hoek-Brown failure criterion

$$n = \frac{1}{2} + \frac{1}{6}\left[\exp\left(-\frac{GSI}{15}\right) - \exp\left(-\frac{20}{3}\right)\right] \tag{4}$$

where m_i is the Hoek-Brown constant of instant rock, D is a disturbance coefficient, and GSI is geological strength index that depends on geological environment, rock structural features and surface characteristic.

A limit load computed from a convex failure surface, which always circumscribes the actual nonlinear failure surface, will be an upper bound on the actual limit load. This is due to the fact that the strength of the convex failure surface is equal to or larger than that of the actual failure surface. By introducing tangential technique into limit analysis, Collins *et al.* (1998), and Drescher and Christopoulos (1988) used tangential line instead of curve to solve this problem successfully. The tangential line to the curve at location of tangency point M, is shown in Fig. 1. The tangential line is described by following equation (Zhang and Chen 1987)

$$\tau = c_t + \sigma_n \tan\varphi_t \tag{5}$$

where φ_t and c_t are the tangential friction angle and the intercept of the straight line with τ-axis respectively. c_t takes the following form (Sun and Zhang 2012, Sun and Liang 2013, Sun and Qin 2014)

$$\frac{c_t}{\sigma_c} = \frac{\cos\varphi_t}{2}\left[\frac{mn(1-\sin\varphi_t)}{2\sin\varphi_t}\right]^{\frac{1}{1-n}} - \frac{\tan\varphi_t}{m}\left(1+\frac{\sin\varphi_t}{n}\right)\left[\frac{mn(1-\sin\varphi_t)}{2\sin\varphi_t}\right]^{\frac{1}{1-n}} + \frac{s}{m}\tan\varphi_t \tag{6}$$

From Fig. 1, it can be seen that the strength of the tangential line equals or exceeds that of the nonlinear yield criterion at the same normal stress. Thus, the linear yield criterion represented by the tangential line will give an upper bound on the actual load for the material, whose failure is governed by the nonlinear yield criterion. In the following part, the tangential line is employed to calculate the rate of external work and internal energy dissipation.

3. Kinematical analysis of 3D rock slope

A homogenous rock slope with angles α and β is considered in the present study, as shown in
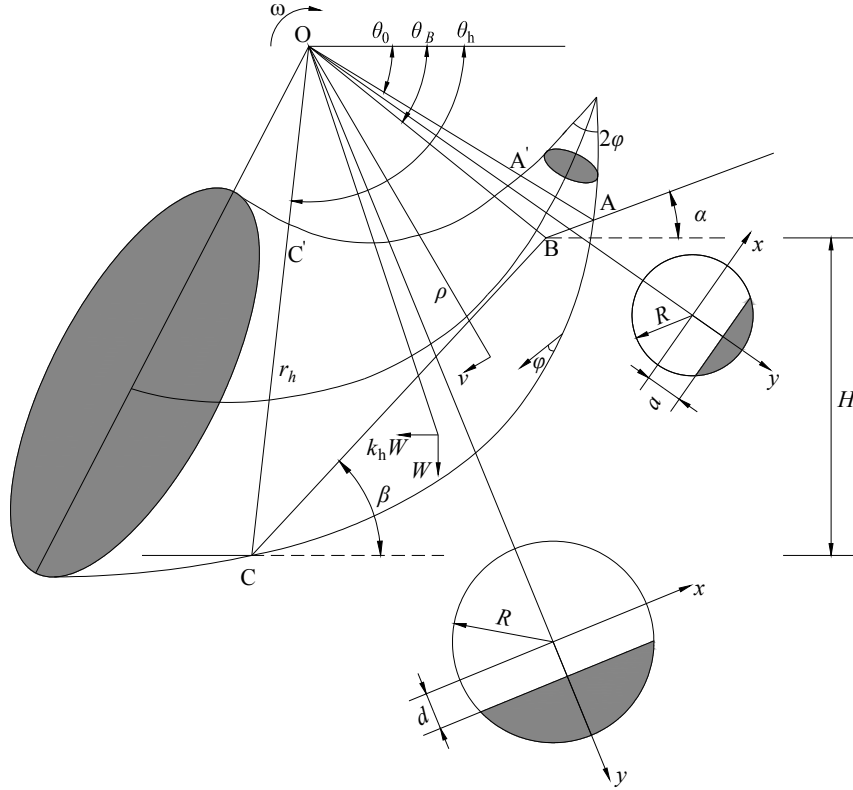
Fig. 2 Three-dimensional rotational mechanism (Michalowski and Drescher 2009) of slope with
       inclined angle

Fig. 2. The slope is subjected to earthquake forces, which is described by a seismic coefficient.
The earthquake forces are regarded as external forces, and the rock masses of the slopes are rigid.
The internal energy is only dissipated along sliding surface, while the external rate of work is done
by the rock weight and earthquake forces. The 3D failure mechanism proposed by Michalowski
and Drescher (2009) is employed in the present limit analysis. Therefore, the following derivation
and some equations are same as those of Michalowski and Drescher (2009). Others are improved,
since the nonlinear HB failure criterion, earthquake forces, and inclined angle α are considered in
the present analysis. For the sake of completeness, those expressions are all reported in the
Appendix of this paper.

3.1 Description of 3D failure mechanism

The 3D failure mechanism proposed by Michalowski and Drescher (2009) has the shape of a
curvilinear cone with apex angle, as shown in Fig. 2. Only a portion of this failure mechanism
intersects the slope, and has one symmetry plane passing the toe point C. The discontinuity surface
on the symmetry plane is described by two log-spirals

$$r = r_0 e^{(\theta - \theta_0)\tan\varphi_t} \tag{7}$$

$$r' = r_0' e^{-(\theta - \theta_0)\tan\varphi_t} \tag{8}$$

where OA $= r_0$, O'A' $= r_0'$. The cross-section of cone is circle of radius R, and the distance between axis of cone and rotation center O is r_m. R and r_m vary with θ

$$r_m = (r + r')/2 = r_0 f_1(\theta) \tag{9}$$

$$R = (r - r')/2 = r_0 f_2(\theta) \tag{10}$$

where the expressions for f_1 and f_2 are reported in the Appendix of this paper.

In above 3D rotation failure mechanism, the critical height is determined by three independent variables $\theta_0 \theta_h$ and r_0'/r_0. Calculations for the mechanism in Fig. 3(a) have shown the minimum stability factor. Previous experience has shown that critical height is related with the width of sliding block, not only with slope angle and strength parameter (Michalowski and Drescher 2009). To make the result consistent with practice, the three-dimensional failure patterns are modified
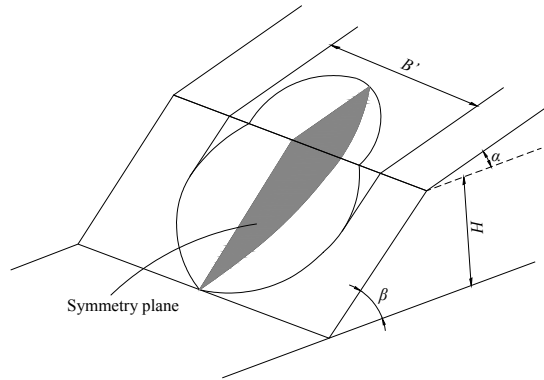
(a) Three-dimensional rotational mechanism with inclined angle
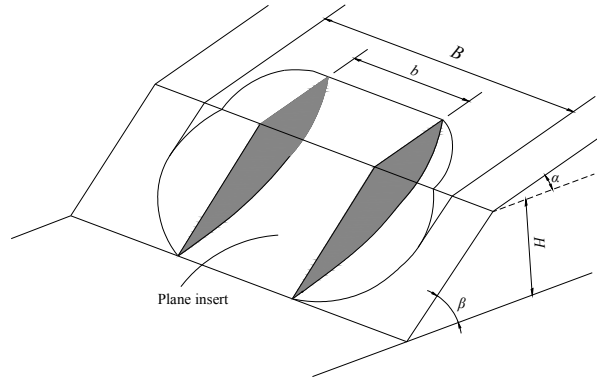
(b) Three-dimensional mechanism with plane insert

Fig. 3 Schematic diagram of three-dimensional mechanism (Michalowski and Drescher 2009) with inclined angle

with a plane insert, by splitting and separating laterally the halves of the 3D surface, as illustrated in Fig. 3(b).

The introduction of plane insert adds a variable b in the optimization of critical height. The sum of rotational mechanism width and plane insert mechanism subject to a limitation imposed on the aximum of slope width. The external work rate and internal energy dissipation of rotating mechanism and plant insert are calculated separately, and the former of which needs complicated integral, while the latter can be obtained by the product of insert width b and those of 2D situation.

3.2 Calculations of external work rate

A local coordinate system x, y is introduced, as shown in Fig. 2. The work rate of rock weight for rotation mechanism is (Michalowski and Drescher 2009)

$$W_{r-3D} = 2\omega\gamma\left[\int_{\theta_0}^{\theta_B}\int_0^{x_1^*}\int_a^{y^*}(r_m+y)^2\cos\theta dxdyd\theta + \int_{\theta_B}^{\theta_h}\int_0^{x_2^*}\int_d^{y^*}(r_m+y)^2\cos\theta dxdyd\theta\right] \tag{11}$$

where ω is the angular velocity, and γ is the unit weight of rock masses. $x_1^* = \sqrt{R^2-a^2}$, $x_2^* = \sqrt{R^2-d^2}$, $y^* = \sqrt{R^2-x^2}$, a and d are found from the geometrical relations

$$a = \frac{\sin(\theta_0+\alpha)}{\sin(\theta+\alpha)}r_0 - r_m = r_0 f_3(\theta) \tag{12}$$

$$d = \frac{\sin(\theta_h+\beta)}{\sin(\theta+\beta)}r_0 e^{(\theta_h-\theta_0)\tan\varphi} - r_m = r_0 f_4(\theta) \tag{13}$$

Angle θ_B is found from the geometrical relations

$$\theta_B = \arctan\frac{\sin(\theta_0+\alpha)}{\cos(\theta_0+\alpha)-\kappa} - \alpha \tag{14}$$

$$\kappa = \frac{\sin(\theta_h-\theta_0)}{\sin\theta_h} - \frac{e^{(\theta_h-\theta_0)\tan\varphi_t}\sin\theta_h - \sin\theta_0}{\sin\theta_h\sin\beta}\sin(\theta_h+\beta) \tag{15}$$

Integration in Eq. (11) is performed analytically with respect to y and x, and only integration over θ is evaluated using a numerical method. Thus, Eq. (11) is

$$W_{\gamma-3D} = \gamma\omega r_0^4 g_1(\theta_0,\theta_h,r_0'/r_0) \tag{16}$$

The work rate of weight for plane insert mechanism is similar with that of plane strain condition. It need multiply the width b. It is expressed as

$$W_{\gamma-insert} = \gamma\omega r_0^4 g_2(\theta_0,\theta_h,b/H) \tag{17}$$

Previous research shows that in most earthquake zones, the vertical acceleration effect is only 40-50% of the horizontal one, so only the horizontal seismic coefficient k_h is considered in the

present study, which is in the range of 0.0 to 0.2. The work rate of rotation mechanism due to earthquake forces is expressed as

$$W_{k_h-3D} = \int_V v_i \gamma_g dV = 2k_h \omega \gamma \left[\int_{\theta_0}^{\theta_B} \int_0^{x_1^*} \int_a^{y^*} (r_m + y)^2 \cos\theta dx dy d\theta + \int_{\theta_B}^{\theta_h} \int_0^{x_2^*} \int_d^{y^*} (r_m + y)^2 \cos\theta dx dy d\theta \right] \quad (18)$$

Eq. (18) can be written as

$$W_{k_h-3D} = \gamma \omega k_h r_0^4 g_3(\theta_0, \theta_h, r_0'/r_0) \quad (19)$$

The work rate of plane insert mechanism due to earthquake can be expressed as

$$W_{k_h-insert} = \gamma \omega k_h r_0^4 g_4(\theta_0, \theta_h, b/H) \quad (20)$$

Thus the external work rate of total failure mechanism can be expressed as

$$W = W_{\gamma-3D} + W_{\gamma-insert} + W_{k_h-3D} + W_{k_h-insert} \quad (21)$$

3.3 Calculations of internal energy dissipation

The work dissipation rate can be more specifically written as the integrals over the surface at the top of the slope and the face of the slope, indicated by D_{AB} and D_{BC} respectively. The internal energy dissipation can be expressed as

$$D_{AB-3D} = -2\omega c_t \cot \varphi_t \int_{\theta_0}^{\theta_B} \int_0^{x_1^*} \frac{\sin^2(\theta_0 + \alpha)}{\sin^3(\theta + \alpha)} \cos(\theta + \alpha) r_0^2 dx d\theta \quad (22)$$

$$D_{BC-3D} = -2\omega c_t \cot \varphi_t \int_{\theta_B}^{\theta_h} \int_0^{x_2^*} \frac{\sin^2(\theta_h + \beta)}{\sin^3(\theta + \beta)} \cos(\theta + \beta) r_0^2 e^{2(\theta_h - \theta_0)\tan \varphi_t} dx d\theta \quad (23)$$

Thus the total rate of energy dissipation of rotation mechanism is

$$D_{3D} = D_{AB-3D} + D_{BC-3D} \quad (24)$$

Eq. (24) can be also written as

$$D_{3D} = \omega c_t \cot \varphi_t r_0^3 g_5(\theta_0, \theta_h, r_0'/r_0) \quad (25)$$

The energy dissipation of plane strain insert can expressed as

$$D_{AB-insert} = -2\omega c_t \cot \varphi_t \int_{\theta_0}^{\theta_B} \int_0^{b/2} \frac{\sin^2(\theta_0 + \alpha)}{\sin^3(\theta + \alpha)} \cos(\theta + \alpha) r_0^2 dx d\theta \quad (26)$$

$$D_{BC-insert} = -2\omega c_t \cot \varphi_t \int_{\theta_B}^{\theta_h} \int_0^{b/2} \frac{\sin^2(\theta_h + \beta)}{\sin^3(\theta + \beta)} \cos(\theta + \beta) r_0^2 e^{2(\theta_h - \theta_0)\tan \varphi_t} dx d\theta \quad (27)$$

Thus, the total energy dissipation of plane insert is

$$D_{insert} = D_{AB-insert} + D_{BC-insert} \tag{28}$$

Eq. (28) can also be written as

$$D_{insert} = \omega c_t \cot \varphi_t r_0^3 g_6(\theta_0, \theta_h, b/H) \tag{29}$$

The formulations of $f_1(\theta) - f_4(\theta)$ and $g_1(\theta_0, \theta_h, b/H) - g_6(\theta_0, \theta_h, b/H)$ are presented in the Appendix. Thus the total rate of work dissipation of failure mechanism is

$$D = D_{3D} + D_{insert} \tag{30}$$

Equating internal energy dissipation to external work rate, the critical height of rock slope under earthquake forces can be obtained

$$H = \frac{c_t \cot \varphi_t \sin \beta}{\gamma \sin(\beta - \alpha)} \left[\sin(\theta_h + \alpha)e^{(\theta_h - \theta_0)\tan \varphi_t} - \sin(\theta_0 + \alpha) \right] \\ \times \frac{g_5(\theta_0, \theta_h, r_0'/r_0) + g_6(\theta_0, \theta_h, b/H)}{g_1(\theta_0, \theta_h, r_0'/r_0) + g_2(\theta_0, \theta_h, b/H) + k_h g_3(\theta_0, \theta_h, r_0'/r_0) + k_h g_4(\theta_0, \theta_h, b/H)} \tag{31}$$

where c_t is determined by Eq. (6). The minimum upper solution of 3D seismic critical height of rock slope is obtained by optimization to Eq. (31).

3.4 Optimization for slope stability factor

Based on nonlinear HB failure criterion, cirtial height of rock slope under earthquake forces is related to these parameters: θ_0, θ_h, r_0'/r_0, b/H, φ_t. In order to make failure mechanism have geometric meaning, the above paramters must satisfy the following constraint conditions.

$$\begin{cases} 0 < \theta_0 < \pi \\ \theta_0 < \theta_h < \pi \\ 0 < r_0'/r_0 < 1 \\ 1 < \varphi_t < \pi/2 \\ 0 < (b + B'_{max})/H < B/H \end{cases} \tag{32}$$

where B'_{max} is the maximum width of rotation mechanism and B is the finite width of slope. When finding the minimum of objective function, the variables are changed sequentially in a single computational loop. The procedure is repeated until the least upper bound solution is obtained. The increments applied to the independent variables are reduced, and the process is repeated. The process is stopped when the increments used in optimisation reached 0.01 for θ_0 and θ_h, and 0.001 for r_0'/r_0, b/H, φ_t.

4. Numerical results

Table 1 Comparison between present stability factors and solutions of Michalowski and Drescher (2009)

B/H		β			
		45°	60°	75°	90°
0.8	Present solutions	63.887	27.085	17.492	12.760
	Michalowski	63.604	27.664	17.827	12.348
1.0	Present solutions	55.822	23.810	14.972	10.825
	Michalowski	54.850	23.835	14.701	11.028
2.0	Present solutions	43.330	18.946	11.874	8.270
	Michalowski	42.732	19.103	12.109	8.604
5.0	Present solutions	38.640	17.088	10.611	7.241
	Michalowski	37.994	17.063	10.628	7.266
10.0	Present solutions	37.331	16.576	10.263	6.961
	Michalowski	36.703	16.527	10.265	6.944

Table 2 The stability factors for $m_i = 7$, $\beta = 60°$, $\alpha = 0°$

k_h	B/H	Parameter GSI							
		10	20	30	40	50	60	70	80
$k_h = 0.00$	0.8	9.91	16.85	18.97	18.21	16.46	14.67	13.04	11.47
	1.0	8.54	14.63	16.48	15.81	14.30	12.74	11.35	9.98
	2.0	7.06	11.97	13.48	12.94	11.70	10.43	9.11	8.02
	5.0	6.33	10.76	12.12	11.63	10.51	9.37	8.15	7.17
	10.0	6.13	10.43	11.75	11.28	10.19	9.08	7.88	6.93
$k_h = 0.05$	0.8	8.07	14.11	16.07	15.42	13.94	12.43	11.18	10.21
	1.0	6.65	11.64	13.56	13.21	11.95	10.64	9.58	8.52
	2.0	5.32	9.32	10.86	10.73	9.70	8.65	7.78	7.01
	5.0	4.87	8.52	9.93	9.78	8.84	7.88	7.09	6.39
	10.0	4.73	8.28	9.64	9.48	8.57	7.64	6.87	6.16
$k_h = 0.10$	0.8	6.76	11.83	13.79	13.38	12.10	10.78	9.70	8.94
	1.0	5.23	9.16	10.67	10.58	9.93	9.12	8.20	7.53
	2.0	4.29	7.51	8.75	8.68	8.14	7.30	6.57	6.05
	5.0	3.94	6.90	8.04	7.97	7.45	6.64	5.98	5.51
	10.0	3.85	6.74	7.85	7.79	7.29	6.50	5.85	5.38
$k_h = 0.15$	0.8	5.82	10.18	11.87	11.77	10.69	9.53	8.57	7.90
	1.0	4.24	7.35	8.80	8.72	8.18	7.63	7.03	6.48
	2.0	3.53	6.12	7.24	7.18	6.73	6.27	5.66	5.21
	5.0	3.18	5.52	6.64	6.62	6.21	5.78	5.23	4.82
	10.0	3.08	5.35	6.43	6.39	5.99	5.59	5.07	4.67

Table 2 Continued

k_h	B/H	Parameter GSI							
		10	20	30	40	50	60	70	80
	0.8	5.06	8.77	10.36	10.27	9.58	8.54	7.68	7.08
	1.0	3.44	5.96	7.18	7.42	6.95	6.96	6.15	5.67
$k_h = 0.20$	2.0	2.72	4.72	5.68	5.88	5.67	5.28	4.97	4.58
	5.0	2.47	4.28	5.15	5.33	5.11	4.77	4.52	4.20
	10.0	2.39	4.15	4.99	5.17	4.95	4.61	4.38	4.05

Table 3 The stability factors for $m_i = 15$, $\beta = 60°$, $\alpha = 15°$

k_h	B/H	Parameter GSI							
		10	20	30	40	50	60	70	80
	0.8	24.32	38.37	40.59	36.94	31.86	26.95	22.72	19.27
	1.0	20.43	32.23	34.73	31.91	27.52	23.28	19.63	16.64
$k_h = 0.00$	2.0	17.11	26.99	28.45	25.89	22.33	18.89	15.93	13.50
	5.0	15.32	24.16	25.76	23.45	20.22	17.10	14.25	12.23
	10.0	14.84	23.41	25.03	22.78	19.65	16.62	14.01	11.88
	0.8	19.63	30.96	33.36	31.00	27.01	22.84	19.26	16.33
	1.0	15.61	25.55	27.53	25.59	22.43	19.30	16.60	14.07
$k_h = 0.05$	2.0	12.81	20.38	21.96	20.41	17.90	15.40	13.25	11.35
	5.0	11.73	18.51	19.95	18.54	16.25	13.93	12.03	10.24
	10.0	11.41	18.00	19.40	18.03	15.80	13.60	11.70	9.95
	0.8	16.45	25.95	27.96	25.98	22.78	19.60	16.71	14.17
	1.0	11.03	18.51	20.69	19.74	17.60	15.14	13.03	11.35
$k_h = 0.10$	2.0	9.34	15.66	17.51	16.40	14.38	12.37	10.64	9.27
	5.0	8.67	14.54	16.16	15.02	13.17	11.33	9.75	8.49
	10.0	8.48	14.23	15.76	14.64	12.84	11.04	9.50	8.28
	0.8	14.16	22.33	24.06	22.36	19.61	16.87	14.52	12.51
	1.0	8.53	14.31	16.00	15.26	13.71	12.13	10.71	9.33
$k_h = 0.15$	2.0	7.07	11.87	13.27	12.66	11.37	10.06	8.79	7.66
	5.0	6.36	10.66	11.92	11.37	10.22	9.04	8.02	6.99
	10.0	6.16	10.34	11.56	11.03	9.91	8.77	7.76	6.76
	0.8	12.43	19.60	21.21	19.63	17.21	14.80	12.74	11.10
	1.0	6.95	11.67	13.04	12.44	11.18	9.89	8.82	7.92
$k_h = 0.20$	2.0	5.44	9.12	10.20	9.73	8.74	7.73	6.90	6.28
	5.0	4.91	8.24	9.21	8.79	7.90	6.99	6.23	5.68
	10.0	4.77	8.00	8.95	8.54	7.67	6.79	6.05	5.51

When $n = 1$, Eq. (1) is written as $\sigma_1 = s\sigma_c + (1 + m)\sigma_3$. Let

$$s\sigma_c = (2c\cos\varphi)/(1 - \sin\varphi) \tag{33}$$

$$1 + m = (1 + \sin\varphi)/(1 - \sin\varphi) \tag{34}$$

Then nonlinear HB failure criterion degenerates to linear MC criterion. With the nonlinear HB failure criterion, the stability factor is defined as

$$N_n = H_c\gamma/(s^{0.5}\sigma_c) \tag{35}$$

4.1 Comparisons

To prove the validity of the present solution, the numerical results, when $n = 1$, $\alpha = 0°$ and $k_h = 0$, are compared with the results of Michalowski and Drescher (2009). In the calculations, $\varphi = 30°$, β varies from 45° to 90°, and $B/H = 0.8, 1.0, 2.0, 5.0, 10.0$. The comparisons are shown in Table 1. From the Table 1, it is found that the maximum difference is less than 4%. The agreement shows that the present method is an effective approach to estimate the 3D stability of rock slopes.

4.2 Design tables

According to upper bound theorem, the stability factor N_n satisfying kinematical admissible condition is the best solution for this failure mechanism.

The strength parameters in HB failure criterion vary with the magnitude GSI, and earthquake forces may affect the stability of rock slopes. Tables 2-3 present the values of seismic and static stability factors for two types of rock, with the parameters $\beta = 60°$, $\alpha = 15°$, $D = 0$, and k_h varying from 0.00 to 0.20, respectively.

From the Tables 2-3, it is found that and the k_h, B/H, and GSI have great influence on rock slope stability. Numerical results are presented for practical use in rock engineering.

5. Conclusions

The upper bound theorem of limit analysis is applied to the seismic and static stability problem of rock slopes with the modified HB failure criterion, employing the 3D failure mechanism proposed by Michalowski and Drescher (2009). With the generalized tangential technique, a linear failure criterion that is tangential to the actual modified HB failure criterion is used to calculate the rate of external work and internal energy dissipation. Equating the work rate of external forces to the internal energy dissipation rate, the objective function is presented. The upper function is obtained by minimizing the objective function with respect to θ_0, θ_h, r'_0/r_0, b/H, φ_t. Based on the analysis above, the conclusions are drawn:

(1) When $n = 1$, the nonlinear HB failure reduces to a linear MC failure criterion, and the static calculation results agree well with solutions of Michalowski and Drescher (2009), with the maximum difference being less than 4%. The agreement shows that the present method is an effective approach to estimate the 3D stability of rock slopes. This paper extends the static 3D stability calculation by Michalowski and Drescher (2009) using a

linear MC failure criterion to seismic analysis using the nonlinear HB failure criterion under earthquake forces.

(2) Based on upper bound theorem, the proposed method is an effective technique for evaluating the 3D stability of rock slopes with nonlinear yield criterion. Due to the usage of the tangential line, the proposed method retains the advantages of kinematical approach, and avoids the difficulty of the calculation of external work rate and energy dissipation rate for varying φ_t. Numerical results for different GSI rock slopes are presented for practical use in rock engineering.

Acknowledgments

References

Agar, J.G., Morgenstern, N.R. and Scott, J. (1985), "Shear strength and stress-strain behavior of Athabasca oil sand at elevated temperatures and pressure", *Can. Geotech. J.*, **24**(1), 1-10.

Baker, R. and Frydman, S. (1983), "Upper bound limit analysis of soil with nonlinear failure criterion", *Soils Found.*, **23**(4), 34-42.

Baligh, M.M. and Azzouz, A.S. (1975), "End effects on stability of cohesive slopes", *J. Geotech. Eng. Div.*, **101**(11), 1105-1117.

Cai, M. (2007), "Back-analysis of rock mass strength parameters using AE monitoring data", *Int. J. Rock Mech. Min. Sci.*, **44**(4), 538-549.

Cai, M., Kaiser, P.K., Tasaka, Y. and Minami, M. (2007), "Determination of residual strength of jointed rock masses using the GSI system", *Int. J. Rock Mech. Min. Sci.*, **44**(2), 247-265.

Collins, I.F., Gunn, C.I., Pender, M.J. and Yan, W. (1998), "Slope stability analyses for materials with nonlinear failure envelope", *Int. J. Numer. Anal. Met. Geomech.*, **12**(6), 533-550.

Drescher, A. and Christopoulos, C. (1988), "Limit analysis slope stability with nonlinear yield condition", *Int. J. Numer. Anal. Met. Geomech*, **12**(3), 341-345.

Farzaneh, O. and Askari, F. (2003), "Three-dimensional analysis of nonhomogeneous slopes", *J. Geotech. Geoenviron. Eng.*, **129**(2), 137-145.

Hobbs, D.W. (1966), "A study of the behaviour of a broken rock under triaxial compression, and its application to mine roadways", *Int. J. Rock Mech. Min. Sci. Geomech. Abstracts*, **3**(1), 11-43.

Hoek, E. and Brown, E.T. (1980), "Empirical strength criterion for rock masses", *J. Geotech. Geoenviron. Eng.*, **106**(9), 1013-1035.

Hoek, E. and Brown, E.T. (1997), "Practical estimate the rock mass strength", *Int. J. Rock Mech. Min. Sci.*, **34**(8), 1165-1186.

Hoek, E., Carranze-Torres, C. and Corkum, B. (2002), *Hoek-Brown Failure Criterion*, (2002 Edition), *Proceedings of the North American Rock Mechanics Society Meeting*, pp. 267-273.

Ladanyi, B. (1974), "Use of the long-term strength concept in the determination of ground pressure of tunnel lining", *Proceeding of the 3rd Congress of International Society of Rock Mechanism on Advances in Rock Mechanism*, National Academy of Science, Washington, D.C., USA, 2B, pp. 1150-1156.

Lade, P.V. (1977), "Elasto-plastic stress-strain theory for cohesionless soil with curved yield surfaces", *Int. J. Solids Struct.*, **13**(11), 1019-1035.

Michalowski, R.L. (1989), "Three-dimensional analysis of locally loaded slopes", *Geotechnique*, **39**(1),

27-38.

Michalowski, R.L. and Drescher, A. (2009), "Three-dimensional stability of slopes and excavations", *Geotechnique*, **59**(10), 839-850.

Sun, Z.B. and Liang, Q. (2013), "Back analysis of general slope under earthquake forces using upper bound theorem", *J. Central South Univ.*, **20**(11), 3274-3281.

Sun, Z.B. and Qin, C.B. (2014), "Stability analysis for natural slope by a kinematical approach", *J. Central South Univ.*, **21**(4), 1546–1553.

Sun, Z.B. and Zhang, D.B. (2012), "Back analysis for slope based on measuring inclination data", *J. Central South Univ.*, **19**(11), 3291-3298.

Zhang, X.J. and Chen, W.F. (1987), "Stability analysis of slopes with general nonlinear failure criterion", *Int. J. Numer. Anal. Met. Geomech.*, **11**(1), 33-50.

Zhang, C.C., Xu, Q. and Zhu, H.H. (2014), "Evaluations of load-deformation behavior of soil nail using hyperbolic pullout model", *Geomech. Eng., Int. J.*, **6**(3), 277-292.

Zhu, H.H., Yin, J.H. and Dong, J.H. (2010), "Physical modelling of sliding failure of concrete gravity dam under overloading condition", *Geomech. Eng., Int. J.*, **2**(2), 89-106.

Zhu, H.H., Yin, J.H. and Yeung, A.T. (2011), "Field Pullout Testing and Performance Evaluation of GFRP Soil Nails", *J. Geotech. Geoenviron. Eng.*, **137**(7), 633-642.

Zhu, H.H., Ho, N.L. and Yin, J.H. (2012), "An optical fibre monitoring system for evaluating the performance of a soil nailed slope", *Smart Struct. Syst., Int. J.*, **9**(5), 393-410.

CC

Appendix

$$\frac{H}{r_0} = \frac{\sin\beta}{\sin(\beta - \alpha)}[\sin(\theta_h + \alpha)e^{(\theta_h - \theta_0)\tan\varphi_t} - \sin(\theta_0 + \alpha)] \tag{A1}$$

$$\frac{L}{r_0} = \frac{\sin(\theta_h - \theta_0)}{\sin(\theta_h + \alpha)} - \frac{\sin(\theta_h + \beta)}{\sin(\theta_h + \alpha)\sin(\beta - \alpha)}[\sin(\theta_h + \alpha)e^{(\theta_h - \theta_0)\tan\varphi_t} - \sin(\theta_0 + \alpha)] \tag{A2}$$

$$f_1(\theta) = \frac{1}{2}[e^{(\theta - \theta_0)\tan\varphi_t} + \frac{r_0'}{r_0}e^{-(\theta - \theta_0)\tan\varphi_t}] \tag{A3}$$

$$f_2(\theta) = \frac{1}{2}[e^{(\theta - \theta_0)\tan\varphi_t} - \frac{r_0'}{r_0}e^{-(\theta - \theta_0)\tan\varphi_t}] \tag{A4}$$

$$f_3(\theta) = \frac{\sin(\theta_0 + \alpha)}{\sin(\theta + \alpha)} - \frac{1}{2}[e^{(\theta - \theta_0)\tan\varphi_t} + \frac{r_0'}{r_0}e^{-(\theta - \theta_0)\tan\varphi_t}] \tag{A5}$$

$$f_4(\theta) = \frac{\sin(\theta_h + \beta)}{\sin(\theta + \beta)}e^{(\theta_h - \theta_0)\tan\varphi} - \frac{1}{2}[e^{(\theta - \theta_0)\tan\varphi_t} + \frac{r_0'}{r_0}e^{-(\theta - \theta_0)\tan\varphi_t}] \tag{A6}$$

$$\begin{aligned} g_1(\theta_0, \theta_h, r_0'/r_0) = &2\int_{\theta_0}^{\theta_B}[(f_2^2 f_3/8 - f_3^3/4 - 2f_1 f_3^2/3 - f_3 f_1^2/2 + 2f_1 f_2^2/3)\sqrt{f_2^2 - f_3^2} \\ &+ (f_2^4/8 + f_2^2 f_1^2/2)\arcsin(\sqrt{f_2^2 - f_3^2}/f_2)]\cos\theta d\theta \\ &+ 2\int_{\theta_B}^{\theta_h}[(f_2^2 f_4/8 - f_4^3/4 - 2f_1 f_4^2/3 - f_4 f_1^2/2 + 2f_1 f_2^2/3)\sqrt{f_2^2 - f_4^2} \\ &+ (f_2^4/8 + f_2^2 f_1^2/2)\arcsin(\sqrt{f_2^2 - f_4^2}/f_2)]\cos\theta d\theta \end{aligned} \tag{A7}$$

$$f_5(\theta_0, \theta_h) = \frac{1}{3(1 + 9\tan^2\varphi_t)}[(3\tan\varphi\cos\theta_h + \sin\theta_h)e^{3(\theta_h - \theta_0)\tan\varphi_t} - (3\tan\varphi\cos\theta_0 + \sin\theta_0)] \tag{A8}$$

$$f_6(\theta_0, \theta_h) = \frac{1}{6}\frac{L}{r_0}(2\cos\theta_0 - \frac{L}{r_0}\cos\alpha)\sin(\theta_0 + \alpha) \tag{A9}$$

$$f_7(\theta_0, \theta_h) = \frac{1}{6}e^{(\theta_h - \theta_0)\tan\varphi_t}[\sin(\theta_h - \theta_0) - \frac{L}{r_0}\sin(\theta_h + \alpha)][\cos\theta_0 - \frac{L}{r_0}\cos\alpha + \cos\theta_h e^{(\theta_h - \theta_0)\tan\varphi_t}] \tag{A10}$$

$$g_2(\theta_0, \theta_h, b/H) = \frac{b}{H}(f_5 - f_6 - f_7)\frac{\sin\beta}{\sin(\beta - \alpha)}[\sin(\theta_h + \alpha)e^{(\theta_h - \theta_0)\tan\varphi_t} - \sin(\theta_0 + \alpha)] \tag{A11}$$

$$g_3(\theta_0,\theta_h,r_0'/r_0)=2\int_{\theta_0}^{\theta_B}[(f_2^2 f_3/8-f_3^3/4-2f_1 f_3^2/3-f_3 f_1^2/2+2f_1 f_2^2/3)\sqrt{f_2^2-f_3^2}$$
$$+(f_2^4/8+f_2^2 f_1^2/2)\arcsin(\sqrt{f_2^2-f_3^2}/f_2)]\sin\theta d\theta$$
$$+2\int_{\theta_B}^{\theta_h}[(f_2^2 f_4/8-f_4^3/4-2f_1 f_4^2/3-f_4 f_1^2/2+2f_1 f_2^2/3)\sqrt{f_2^2-f_4^2}$$
$$+(f_2^4/8+f_2^2 f_1^2/2)\arcsin(\sqrt{f_2^2-f_4^2}/f_2)]\sin\theta d\theta \quad\quad (A12)$$

$$f_8(\theta_0,\theta_h)=\frac{1}{3(1+9\tan^2\varphi_t)}[(3\tan\varphi_t\sin\theta_h-\cos\theta_h)e^{3(\theta_h-\theta_0)\tan\varphi_t}-(3\tan\varphi_t\sin\theta_0-\cos\theta_0)] \quad\quad (A13)$$

$$f_9(\theta_0,\theta_h)=\frac{1}{6}\frac{L}{r_0}(2\sin\theta_0+\frac{L}{r_0}\sin\alpha)\sin(\theta_0+\alpha) \quad\quad (A14)$$

$$f_{10}(\theta_0,\theta_h)=\frac{1}{6}e^{(\theta_h-\theta_0)\tan\varphi_t}\frac{H}{r_0}\frac{\sin(\theta_h+\beta)}{\sin\beta}[2\sin\theta_h e^{(\theta_h-\theta_0)\tan\varphi_t}-\frac{H}{r_0}] \quad\quad (A15)$$

$$g_4(\theta_0,\theta_h,b/H)=\frac{b}{H}(f_8-f_9-f_{10})\frac{\sin\beta}{\sin(\beta-\alpha)}[\sin(\theta_h+\alpha)e^{(\theta_h-\theta_0)\tan\varphi_t}-\sin(\theta_0+\alpha)] \quad\quad (A16)$$

$$g_5(\theta_0,\theta_h,r_0'/r_0)=-2\sin^2(\theta_0+\alpha)\int_{\theta_0}^{\theta_B}\frac{\cos(\theta+\alpha)}{\sin^3(\theta+\alpha)}\sqrt{f_2^2-f_3^2}d\theta$$
$$-2e^{2(\theta_h-\theta_0)\tan\varphi_t}\sin^2(\theta_h+\beta)\int_{\theta_B}^{\theta_h}\frac{\cos(\theta+\beta)}{\sin^3(\theta+\beta)}\sqrt{f_2^2-f_4^2}d\theta \quad\quad (A17)$$

$$g_6(\theta_0,\theta_h,b/H)=\frac{b}{2H}\{\frac{\sin^2(\theta_0+\alpha)}{\sin^2(\theta_B+\alpha)}-1+[1-\frac{\sin^2(\theta_h+\beta)}{\sin^2(\theta_B+\beta)}]e^{2(\theta_h-\theta_0)\tan\varphi_t}\}$$
$$\cdot\frac{\sin\beta}{\sin(\beta-\alpha)}[\sin(\theta_h+\alpha)e^{(\theta_h-\theta_0)\tan\varphi_t}-\sin(\theta_0+\alpha)] \quad\quad (A18)$$